DOI 10.1007/s10778-025-01339-4
International Applied Mechanics, Vol. 61, No. 1, January, 2025

ON INFLUENCE OF FLUID VISCOSITY ON INTERFACE PRESSURE IN HYDRO-PIEZOELECTRIC SYSTEM UNDER ITS FORCED VIBRATION*

S. D. Akbarov[1,2] and Z. Ekicioglu Kuzeci[3]

The primary focus of this paper is to examine the effect of fluid viscosity on vibration that occurs when harmonic mechanical force is applied to a system consisting of a piezoelectric plate, a compressible viscous fluid, and a rigid wall. The exact equations of motion of the linear electro-elasticity theory for the piezoelectric materials are used to describe the plate motion. The plane-strain state of the plate is considered. The linearized Navier-Stokes equations for a compressible (barotropic) viscous fluid are used to describe the fluid flow, and the plane flow is taken into consideration. Equations corresponding to the problem are solved by applying the Fourier transform with respect to the space coordinate, which is on the coordinate axis directed along the plate-lying direction. The Fourier transforms are determined analytically, but the inverse transforms are computed numerically. Numerical results on the interface pressure are obtained for the PMN-PT and PZT-2 materials, and the results are discussed. According to these results, it is established that the fluid viscosity causes the increase in the amplitude of the interface normal stress and can also significantly affect the vibration phase at which the studied stress has its absolute minimum value. Furthermore, the electromechanical coupling effects of the plate material on the studied parameters are determined.

Keywords: piezoelectric plate, forced vibration, fluid viscosity, compressible viscous fluid, coupling effect

1. Introduction. In the literature, the study of plate and fluid interaction has a long history that starts with the work of Lamb [1]; afterwards, many further studies have been conducted on this subject. A thorough review of the history of this topic can be found in the studies of Amabili [2], Akbarov [3], Akbarov and Ismailov [4], Guz [5], Guz, Zhuk, and Bagno [6], Paimushin and Gazizullin [7], Paimushin et al. [8], Shuaib et al. [9], Sorokin and Chubinskij [10], Zamanov et al. [11], and many others listed therein. These investigations can be classified into three aspects: first, according to theories applied to describe the motion of the plate; second, according to the type of dynamic problem (wave dispersion, free vibration, and forced vibration); and at last, according to defined fluid modeling (inviscid fluid, viscous fluid, compressible fluid, and incompressible fluid). There are studies in which the fluid is modeled as the inviscid fluid [12–16]. However, studies considering the fluid as viscous in interaction problems are also given in [17–21].

[1]Department of Mechanical Engineering, Yildiz Technical University, 34349, Besiktas, Istanbul, Turkiye; e-mail: akbarov@yildiz.edu.tr; [2]Institute of Mathematics and Mechanics of Science and Education Ministry Republic of Azerbaijan, Baku, Azerbaijan Az141; [3]Department of Mechanical Engineering, Kirsehir Ahi Evran University, 40100, Kirsehir, Turkiye; e-mail: zeynep.kuzeci@ahievran.edu.tr. Translated from Prykladna Mekhanika, Vol. 61, No. 1, pp. 132–144, January–February 2025. Original article submitted October 31, 2023.

* Based on the materials of the report at the International Scientific Conference *Modern Problems of Mechanics—2023* dedicated to the 145th anniversary of S. P. Timoshenko, Kyiv, November 14–16, 2023.

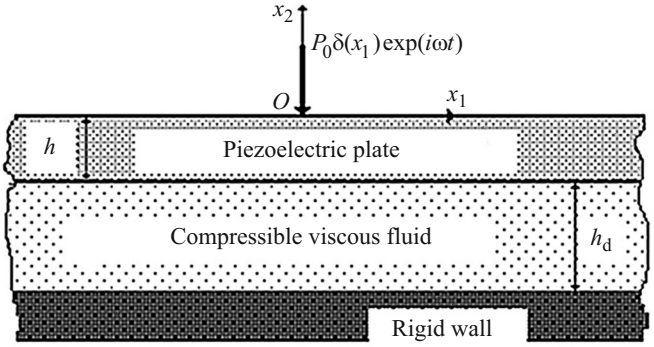

Fig. 1. Sketch of system.

2. Formulation of Problem. Study on the forced vibration of the hydro-piezoelectric system consisting of a piezoelectric plate, a compressible fluid and a rigid wall has been performed in [22]. Investigations is expanded for the influence of the fluid viscosity to the stress on the plate-fluid interface in this annotation. The system is shown in Fig. 1. According to this figure, h is the piezoelectric plate thickness, h_d is the fluid depth, respectively. The plate occupy the regions $\{-\infty < x_1 < +\infty, -h < x_2 < 0, -\infty < x_3 < +\infty\}$ and the fluid occupies the region $\{-\infty < x_1 < +\infty, -h - h_d < x_2 < -h, -\infty < x_3 < +\infty\}$. Also, the Cartesian coordinate system $Ox_1x_2x_3$ on the upper surface plane of the plate is defined and Ox_3 axis is perpendicular to the figure plane. The plane strain state in the plate and the two-dimensional flow of the fluid on the plane Ox_1x_2 are considered. Furthermore, it is assumed that the homogeneous time-harmonic linear mechanical force with intensity P_0 is applied at the upper surface of the plate.

In the problem mathematical formulation, the equations of the motion of the piezoelectric plate and the constitutive equations are given in (1) and (2), respectively

$$\frac{\partial \sigma_{11}}{\partial x_1} + \frac{\partial \sigma_{12}}{\partial x_2} = \rho \frac{\partial^2 u_1}{\partial t^2}, \qquad \frac{\partial \sigma_{12}}{\partial x_1} + \frac{\partial \sigma_{22}}{\partial x_2} = \rho \frac{\partial^2 u_2}{\partial t^2}, \qquad \frac{\partial D_1}{\partial x_1} + \frac{\partial D_2}{\partial x_2} = 0. \tag{1}$$

$$\sigma_{11} = c_{11}\gamma_{11} + c_{13}\gamma_{22} - e_{31}E_2, \quad \ldots; \qquad \sigma_{12} = c_{44}(\gamma_{12} + \gamma_{21}) - e_{15}E_1,$$

$$D_1 = e_{15}(\gamma_{12} + \gamma_{21}) + \varepsilon_{11}E_1, \ldots, \tag{2}$$

where

$$\gamma_{11} = \frac{\partial u_1}{\partial x_1}, \qquad \gamma_{22} = \frac{\partial u_2}{\partial x_2}, \qquad \gamma_{21} = \gamma_{12} = \frac{1}{2}\left(\frac{\partial u_1}{\partial x_2} + \frac{\partial u_2}{\partial x_1}\right), \tag{3}$$

where σ_{11}, σ_{12}, and σ_{22} are the components of the mechanical stress tensor in the plane-strain state; u_1 and u_2 are the components of the mechanical displacement vector; γ_{11}, γ_{22}, and γ_{12} are the components of the mechanical strain tensor; D_1 and D_2 are the components of the electrical displacement vector; φ is the electric potential; c_{11}, c_{33}, c_{13}, and c_{44} are the elastic constants; e_{31}, e_{33}, and e_{15} are the piezoelectric constants; ε_{11} and ε_{33} are the dielectric constants. The linearized Navier-Stokes equations defining the fluid flow, the fluid continuity equation, and the linearized rheological relations are given in (4), (5), and (6), respectively

$$\rho_0^{(1)} \frac{\partial V_1}{\partial t} - \mu^{(1)}\left(\frac{\partial^2 V_1}{\partial x_1^2} + \frac{\partial^2 V_1}{\partial x_2^2}\right) + \frac{\partial p^{(1)}}{\partial x_1} - (\mu^{(1)} + \lambda^{(1)})\frac{\partial \theta}{\partial x_1} = 0,$$

$$\rho_0^{(1)} \frac{\partial V_2}{\partial t} - \mu^{(1)}\left(\frac{\partial^2 V_2}{\partial x_1^2} + \frac{\partial^2 V_2}{\partial x_2^2}\right) + \frac{\partial p^{(1)}}{\partial x_2} - (\mu^{(1)} + \lambda^{(1)})\frac{\partial \theta}{\partial x_2} = 0, \tag{4}$$

$$\gamma_{11}\frac{\partial \rho^{(1)}}{\partial t}+\rho_0^{(1)}\left(\frac{\partial V_1}{\partial x_1}+\frac{\partial V_2}{\partial x_2}\right)=0, \tag{5}$$

$$T_{11}=-p^{(1)}+\lambda^{(1)}\theta+2\mu^{(1)}e_{11},\ \ldots; \qquad T_{33}=-p^{(1)}+\lambda^{(1)}\theta, \qquad T_{12}=2\mu^{(1)}e_{12},$$

$$p^{(1)}=a_0^2\rho^{(1)}, \qquad a_0^2=\frac{\partial p_0^{(1)}}{\partial \rho_0^{(1)}}. \tag{6}$$

In fluid field equations, $\rho_0^{(1)}$ is the fluid density before perturbation; $p_0^{(1)}$ is the hydrostatic pressure before perturbation; $\rho^{(1)}$ is the perturbation of the fluid density; $p^{(1)}$ is the perturbation of the pressure; V_1 and V_2 are the components of the fluid flow velocity vector in the directions of the Ox_1 and Ox_2 axes, respectively; T_{ij} and e_{ij} $(ij=11,\ 22,\ 12)$ are the components of the stress and strain velocity tensors in the fluid; a_0 is the sound velocity in the fluid; $\lambda^{(1)}$ and $\mu^{(1)}$ are the coefficients of the fluid viscosity. To the aforementioned equations and relations, the following representations for the velocities V_1 and V_2, and the pressure $p^{(1)}$ are also added

$$V_1=\frac{\partial \varphi^{(1)}}{\partial x_1}+\frac{\partial \psi^{(1)}}{\partial x_2}, \qquad V_2=\frac{\partial \varphi^{(1)}}{\partial x_2}-\frac{\partial \psi^{(1)}}{\partial x_1},$$

$$p^{(1)}=\rho_0^{(1)}\left(\frac{\lambda^{(1)}+2\mu^{(1)}}{\rho_0^{(1)}}\Delta-\frac{\partial}{\partial t}\right)\varphi^{(1)}, \tag{7}$$

when the following equations are satisfied by potentials $\varphi^{(1)}$ and $\psi^{(1)}$:

$$\left[\left(1+\frac{\lambda^{(1)}+2\mu^{(1)}}{a_0^2\rho_0^{(1)}}\frac{\partial}{\partial t}\right)\Delta-\frac{1}{a_0^2}\frac{\partial^2}{\partial t^2}\right]\varphi^{(1)}=0,$$

$$\left(\nu^{(1)}\Delta-\frac{\partial}{\partial t}\right)\psi^{(1)}=0, \qquad \Delta=\frac{\partial^2}{\partial x_1^2}+\frac{\partial^2}{\partial x_2^2}. \tag{8}$$

If we take $p^{(1)}=-(T_{11}+T_{22}+T_{33})/3$, then the expression $\lambda^{(1)}=-2\mu^{(1)}/3$ can be deduced from the rheological relations in (6). Note that the formulation above is written for the case where the fluid is a compressible viscous one. However, this formulation has been changed for the case where the fluid is inviscid. If we take $\mu^{(1)}=\lambda^{(1)}=0$ and $\psi^{(1)}=0$ in the foregoing relations and equations related to the fluid and ignore the compatibility and the impermeability conditions with respect to the velocity V_1, then we obtain the formulation in (9) for the inviscid fluid case

$$\rho_0^{(1)}\left(\frac{\partial V_1}{\partial t}+\frac{\partial p^{(1)}}{\partial x_1}\right)=0, \qquad \rho_0^{(1)}\left(\frac{\partial V_2}{\partial t}+\frac{\partial p^{(1)}}{\partial x_2}\right)=0. \tag{9}$$

The continuity equation is the same as (4) for the inviscid fluid. Equations (10) and (11) show the constitutive equations and the potential equations for the inviscid fluid, respectively

$$T_{11}=T_{22}=T_{33}-p^{(1)}, \tag{10}$$

$$\left[\Delta-\frac{1}{a_0^2}\frac{\partial^2}{\partial t^2}\right]\varphi^{(1)}=0. \tag{11}$$

Additionally, the expression of inviscid fluid velocity and pressure in terms of potential is as follows:

$$V_2 = \frac{\partial \varphi^{(1)}}{\partial x_2}, \qquad p^{(1)} = \rho_0^{(1)} \left(-\frac{\partial \varphi^{(1)}}{\partial t} \right). \tag{12}$$

The last part of the mathematical formulation specifies the boundary, contact, and impermeability conditions. The following conditions are defined to solve the problem: the boundary conditions of the upper surface of the piezoelectric plate are given in (13), the compatibility conditions on the interface plane of the piezoelectric plate and fluid are given in (14), the impermeability conditions on the rigid wall is given in (15), and the boundary conditions for the electrical part is given in (16)

$$\sigma_{21}\big|_{x_2=0} = 0, \qquad \sigma_{22}\big|_{x_2=0} = -P_0 \delta(x_1) e^{i\omega t}, \tag{13}$$

$$\left.\frac{\partial u_1}{\partial t}\right|_{x_2=-h} = V_1\big|_{x_2=-h}, \qquad \left.\frac{\partial u_2}{\partial t}\right|_{x_2=-h} = V_2\big|_{x_2=-h},$$

$$\sigma_{21}\big|_{x_2=-h} = T_{21}\big|_{x_2=-h}, \qquad \sigma_{22}\big|_{x_2=-h} = T_{22}\big|_{x_2=-h}, \tag{14}$$

$$V_1\big|_{x_2=-h-h_d} = 0, \qquad V_2\big|_{x_2=-h-h_d} = 0, \tag{15}$$

$$D_2\big|_{x_2=0} = 0, \qquad D_2\big|_{x_2=-h} = 0. \tag{16}$$

3. Method of Solution. Considering the characteristics of time-dependent harmonic vibration, all investigated parameters of the problem were defined in the form of $g(x_1, x_2, t) = \bar{g}(x_1, x_2) e^{i\omega t}$. Thus, these expressions $\omega(\bullet)$ and $-\omega^2(\bullet)$ were written instead of the derivatives $\partial(\bullet)/\partial t$ and $\partial^2(\bullet)/\partial t^2$. Following this mathematical procedure, the boundary, contact, compatibility, and impermeability equations were used to obtain the amplitudes of the investigated parameters. For the solution of these equations, we employed the exponential Fourier transform that was given in (17). The amplitudes of the investigated parameters were given by (18)

$$f_F(s, x_2) = \int_{-\infty}^{+\infty} f(x_1, x_2) e^{-isx_1} dx_1, \tag{17}$$

$$u_1 = \frac{1}{2\pi} \int_{-\infty}^{\infty} u_{1F}(s, x_2) e^{isx_1} ds, \ldots; \qquad \sigma_{11} = \frac{1}{2\pi} \int_{-\infty}^{\infty} \sigma_{11F}(s, x_2) e^{isx_1} ds, \ldots;$$

$$D_1 = \frac{1}{2\pi} \int_{-\infty}^{\infty} D_{1F}(s, x_2) e^{isx_1} ds, \ldots; \qquad \varphi = \frac{1}{2\pi} \int_{-\infty}^{\infty} \varphi_F(s, x_2) e^{isx_1} ds, \ldots;$$

$$V_1 = \frac{1}{2\pi} \int_{-\infty}^{\infty} V_{1F}(s, x_2) e^{isx_1} ds, \ldots; \qquad T_{11} = \frac{1}{2\pi} \int_{-\infty}^{\infty} T_{11F}(s, x_2) e^{isx_1} ds, \ldots. \tag{18}$$

Thus, by substituting the expressions in (18) into the preceding equations and relations, we obtain the corresponding equations and relations for the amplitude Fourier transforms. First, we consider the procedure for solving these equations for the plate. We can obtain the following system of the ordinary differential equations in (19) for u_{1F}, u_{2F}, and φ_F by using the Fourier transforms of the relations (2) and (3) and performing the corresponding mathematical manipulations

$$\left(\frac{c^2}{s^2} - \tilde{c}_{11} \right) u_{1F} + \frac{d^2 u_{1F}}{d(sx_2)^2} - i(1 + \tilde{c}_{13}) \frac{du_{2F}}{d(sx_2)} - i(1 + \tilde{e}_{31}) \frac{d\tilde{\varphi}_F}{d(sx_2)} = 0,$$

$$-i(1 + \tilde{c}_{13}) \frac{du_{1F}}{d(sx_2)} + \left(\frac{c^2}{s^2} - 1 \right) u_{2F} + \tilde{c}_{33} \frac{d^2 u_{2F}}{d(sx_2)^2} - \tilde{\varphi}_F + \tilde{e}_{33} \frac{d^2 \tilde{\varphi}_F}{d(sx_2)^2} = 0,$$

$$-i(1+\tilde{e}_{31})\frac{du_{1F}}{d(sx_2)}+\tilde{e}_{33}\frac{d^2u_{2F}}{d(sx_2)^2}-u_{2F}+\tilde{\varepsilon}_{11}\tilde{\varphi}_F-\tilde{\varepsilon}_{33}\frac{d\tilde{\varphi}_F}{d(sx_2)}=0, \tag{19}$$

where

$$c^2=\frac{\omega^2h^2}{c_{44}/\rho},\qquad \tilde{c}_{11}=\frac{c_{11}}{c_{44}},\qquad \tilde{c}_{13}=\frac{c_{13}}{c_{44}},\qquad \tilde{e}_{31}=\frac{e_{31}}{e_{15}},\qquad \tilde{c}_{33}=\frac{c_{33}}{c_{44}},$$

$$\tilde{e}_{33}=\frac{e_{33}}{c_{44}},\qquad \tilde{\varphi}_F=\frac{e_{15}}{c_{44}}\varphi_F,\qquad \tilde{\varepsilon}_{11}=\frac{\varepsilon_{11}c_{44}}{e_{15}^2},\qquad \tilde{\varepsilon}_{33}=\frac{\varepsilon_{33}c_{44}}{e_{15}^2}. \tag{20}$$

According to the Euler method, the particular solution of the ordinary differential equation in (19) is given as follows:

$$u_{1F}=iAe^{bsx_2},\qquad u_{2F}=Be^{bsx_2},\qquad \tilde{\varphi}_F=Ce^{bsx_2}. \tag{21}$$

It should be noted that A, B, C and b are the unknown constants that will be calculated in the following section. Then we obtain following system of homogeneous linear algebraic equations with respect to the unknown constants A, B and C by substituting the particular solution in (21) into the system of equations in (19)

$$\left(b^2+\left(\frac{c^2}{s^2}-\tilde{c}_{11}\right)\right)A-(1+\tilde{c}_{13})bB-(1+\tilde{e}_{31})bC=0,$$

$$(1+\tilde{c}_{13})bA+\left(\frac{c^2}{s^2}-1+\tilde{c}_{33}b^2\right)B+(\tilde{e}_{33}b^2-1)C=0,$$

$$(1+\tilde{e}_{31})bA+(\tilde{e}_{33}b^2-1)B+(\tilde{\varepsilon}_{11}-\tilde{\varepsilon}_{33}b^2)C=0. \tag{22}$$

We equalize the determinant of the system's coefficient matrices in order to get the non-trivial solution to the system of equations in (22), and we arrive at the bicubic equation shown below for determining the unknown constant b

$$b_1^3+a_4b_1^2+a_2b_1+a_0=0. \tag{23}$$

The following notation is accepted in (23)

$$b_1=b^2,\ a_4=\left[\tilde{c}_{33}\tilde{\varepsilon}_{11}-\tilde{\varepsilon}_{33}\alpha_{22}-\tilde{\varepsilon}_{33}\alpha_{11}\tilde{c}_{33}-\tilde{e}_{33}\left(\alpha_{21}\alpha_{13}+\alpha_{13}\alpha_{31}\right)\right.$$

$$\left.+\alpha_{13}\alpha_{31}\tilde{c}_{33}-\tilde{\varepsilon}_{33}\alpha_{12}\alpha_{21}-\alpha_{11}\tilde{e}_{33}^2+2\tilde{e}_{33}\right]\left(-\tilde{\varepsilon}_{33}\tilde{c}_{33}-\tilde{e}_{33}^2\right)^{-1},$$

$$a_2=\left[\tilde{\varepsilon}_{11}\alpha_{22}+\tilde{\varepsilon}_{11}\alpha_{11}\tilde{\varepsilon}_{33}-\tilde{\varepsilon}_{33}\alpha_{11}\alpha_{22}+\alpha_{21}\alpha_{13}+\alpha_{12}\alpha_{31}\right.$$

$$\left.+\alpha_{13}\alpha_{31}\alpha_{22}+\tilde{\varepsilon}_{11}\alpha_{12}\alpha_{21}-2\alpha_{11}\tilde{e}_{33}-1\right](-\tilde{\varepsilon}_{33}\tilde{c}_{33}-\tilde{e}_{33}^2)^{-1},$$

$$a_0=[\tilde{\varepsilon}_{11}\alpha_{11}\alpha_{22}-\alpha_{11}](-\tilde{\varepsilon}_{33}\tilde{c}_{33}-\tilde{e}_{33}^2)^{-1}, \tag{24}$$

where

$$\alpha_{11}=\frac{c^2}{s^2}-\tilde{c}_{11},\qquad \alpha_{12}=1+\tilde{c}_{13},\qquad \alpha_{13}=1+\tilde{e}_{31},$$

$$\alpha_{21}=1+\tilde{c}_{13},\qquad \alpha_{22}=\frac{c^2}{s^2}-1,\qquad \alpha_{31}=1+\tilde{e}_{31}. \tag{25}$$

For finding the roots of (23), we employ Vieta's trigonometric formula for cubic equations (detailed information in [22]). After determining the six roots of the bicubic characteristic equation in (23), the general solution to the system of the ordinary differential equation in (22) is written as the expressions in (26)

$$u_{1F} = iA_1 e^{b_1 s x_2} + iA_2 e^{b_2 s x_2} + iA_3 e^{b_3 s x_2} + iA_4 e^{b_4 s x_2} + iA_5 e^{b_5 s x_2} + iA_6 e^{b_6 s x_2},$$

$$u_{2F} = A_1 Y_1 e^{b_1 s x_2} + A_2 Y_2 e^{b_2 s x_2} + A_3 Y_3 e^{b_3 s x_2} + A_4 Y_4 e^{b_4 s x_2} + A_5 Y_5 e^{b_5 s x_2} + A_6 Y_6 e^{b_6 s x_2},$$

$$\varphi_F = A_1 Z_1 e^{b_1 s x_2} + A_2 Z_2 e^{b_2 s x_2} + A_3 Z_3 e^{b_3 s x_2} + A_4 Z_4 e^{b_4 s x_2} + A_5 Z_5 e^{b_5 s x_2} + A_6 Z_6 e^{b_6 s x_2}, \tag{26}$$

where

$$Y_k = \frac{-(b_k + \alpha_{11})(\tilde{\varepsilon}_{11} - \tilde{\varepsilon}_{33} b_k^2) - \alpha_{31}\alpha_{13} b_k^2}{\tilde{e}_{13} b_k (\tilde{e}_{13} b_k^2 - 1) - \alpha_{12} b_k (\tilde{\varepsilon}_{11} - \tilde{\varepsilon}_{13} b_k^2)},$$

$$Z_k = \frac{(b_k^2 + \alpha_{11})(\tilde{e}_{13} b_k^2 - 1) + \alpha_{31}\alpha_{12} b_k^2}{\tilde{e}_{13} b_k (\tilde{e}_{13} b_k^2 - 1) - \alpha_{12} b_k (\tilde{\varepsilon}_{11} - \tilde{\varepsilon}_{13} b_k^2)}. \tag{27}$$

When the expression in (27) is substituted into the Fourier transform of the relationships in (2), the expressions in (28) for the stresses and electrical displacements that enter the boundary and compatibility conditions are obtained

$$\sigma_{12F} = i\sum_{k=1}^{6} (b_k s - s Y_k - s Z_k) e^{b_k s x_2} A_k,$$

$$\sigma_{22F} = \sum_{k=1}^{6} (s c_{11} + c_{13} b_k s Y_k + e_{13} b_k s Z_k) e^{b_k s x_2} A_k,$$

$$D_{2F} = \sum_{k=1}^{6} \left(s e_{13} + b_k s e_{33} Y_k - \varepsilon_{33} \frac{c_{44}}{e_{15}} s b_k Z_k \right) e^{b_k s x_2} A_k. \tag{28}$$

After completing the Fourier transform of the plate expressions, we will attempt to determine the Fourier transforms of fluid flow quantities, beginning with $\varphi_F^{(1)}$ and $\psi_F^{(1)}$, which will be used to determine the Fourier transforms of velocities and pressure. The Fourier transforms of $\varphi_F^{(1)}$ and $\psi_F^{(1)}$ are as follows:

$$\varphi_F^{(1)} = \omega h^2 \tilde{\varphi}_F^{(1)}, \qquad \psi_F^{(1)} = \omega h^2 \tilde{\psi}_F^{(1)}. \tag{29}$$

After some mathematical manipulations and using the Fourier transform of the equations in (8) and the expressions in (29) yield the equations that follow for the functions $\tilde{\varphi}_F^{(1)}$ and $\tilde{\psi}_F^{(1)}$

$$\frac{d^2 \tilde{\varphi}_F^{(1)}}{dx_2^2} + \left(\frac{\Omega_1^2}{1 + i4\Omega_1^2 / (3N_w^2)} - s^2 \right) \tilde{\varphi}_F^{(1)} = 0,$$

$$\frac{d^2 \tilde{\psi}_F^{(1)}}{dx_2^2} - (s^2 + iN_w^2) \tilde{\psi}_F^{(1)} = 0. \tag{30}$$

The expression of the dimensionless numbers in (35), which characterize the effect of the fluid viscosity and fluid compressibility, respectively, is $\Omega_1 = \omega h / a_0$ and $N_w^2 = \omega h^2 / \nu^{(1)}$. It should be noted that the relation $\lambda^{(1)} = -2\mu^{(1)} / 3$ is taken into account when getting the equations in (30). The solution to the equations in (30) is calculated by using the well-known solution technique of the ordinary differential equations and it is presented as follows:

$$\tilde{\varphi}_F^{(1)} = A_7 e^{\delta_1 x_2} + A_8 e^{-\delta_1 x_2},$$

$$\tilde{\psi}_F^{(1)} = A_9 e^{\gamma_1 x_2} + A_{10} e^{-\gamma_1 x_2}, \tag{31}$$

where A_7, A_8, A_9, A_{10} are the unknown constants and $\delta_1 = \sqrt{s^2 - \dfrac{\Omega_1^2}{1 + i4\Omega_1^2 / (3N_w^2)}}$, $\gamma_1 = \sqrt{s^2 + iN_w^2}$.

Using the expressions in (31), (29), (7) and (6), the following expressions are obtained for the quantities related to the fluid flow

$$V_{1F} = \omega h[-A_7 s e^{\delta_1 x_2} - A_8 s e^{-\delta_1 x_2} + A_9 e^{\gamma_1 x_2} + A_{10} e^{-\gamma_1 x_2}],$$

$$V_{2F} = \omega h[A_7 \delta_1 e^{\delta_1 x_2} - A_8 \delta_1 e^{-\delta_1 x_2} - A_9 s e^{\gamma_1 x_2} - A_{10} s e^{-\gamma_1 x_2}],$$

$$T_{22F} = \mu^{(1)} \omega \left[A_7 \left(\frac{4}{3}\delta_1^2 + \frac{2}{3}s^2 - R_0 \right) e^{\delta_1 x_2} + A_8 \left(\frac{4}{3}\delta_1^2 + \frac{2}{3}s^2 - R_0 \right) e^{-\delta_1 x_2} \right.$$

$$\left. + A_9 \left(-s\gamma_1 - \frac{2}{3}s\gamma_1 \right) e^{\gamma_1 x_2} + A_{10} \left(s\gamma_1 + \frac{2}{3}s\gamma_1 \right) e^{-\gamma_1 x_2} \right],$$

$$T_{21F} = -\mu^{(1)} \omega \left[2s\delta_1 A_7 e^{\delta_1 x_2} - 2s\delta_1 A_8 e^{-\delta_1 x_2} + (s^2 + \gamma_1^2) A_9 e^{\gamma_1 x_2} + (s^2 + \gamma_1^2) A_{10} e^{-\gamma_1 x_2} \right],$$

$$p_F^{(1)} = \mu^{(1)} \omega R_0 (A_7 e^{\delta_1 x_2} + A_8 e^{-\delta_1 x_2}), \tag{32}$$

where

$$R_0 = -\frac{4}{3} \frac{\Omega_1^2}{1 + i4\Omega_1^2 / (3N_w^2)} - iN_w^2. \tag{33}$$

Thus, finding the Fourier transforms of the expressions for the plate and fluid that will enter the boundary conditions is completed. Substituting the expressions (26), (28), and (32) into the boundary (16) and (13), compatibility (14), and impermeability (15) conditions, we obtain the system of algebraic equations for the unknown constants A_1, A_2, A_3, A_4, A_5, A_6, A_7, A_8, A_9, and A_{10}. Thus, we obtain ten equations with respect to the ten unknown constants and after determination of these constants from the equations in (34).

$$D_{2F}\big|_{x_2=0} = 0 \Rightarrow \sum_{k=1}^{6} \left(se_{13} + b_k s e_{33} Y_k - \varepsilon_{33} \frac{c_{44}}{e_{15}} s b_k Z_k \right) A_k = 0,$$

$$\sigma_{21F}\big|_{x_2=0} = 0 \Rightarrow i \sum_{k=1}^{6} (b_k s - sY_k - sZ_k) A_k = 0,$$

$$\sigma_{22F}\big|_{x_2=0} = -P_0 \Rightarrow \sum_{k=1}^{6} (sc_{11} + c_{13} b_k s Y_k + e_{13} b_k s Z_k) A_k = 0,$$

$$\sigma_{21F}\big|_{x_2=-h} - T_{21F}\big|_{x_2=-h} = 0 \Rightarrow i \sum_{k=1}^{6} (b_k s - sY_k - sZ_k) e^{-b_k sh} A_k$$

$$+ \mu^{(1)} \omega \left[2s\delta_1 A_7 e^{-\delta_1 h} - 2s\delta_1 A_8 e^{+\delta_1 h} + (s^2 + \gamma_1^2) A_9 e^{-\gamma_1 h} + (s^2 + \gamma_1^2) A_{10} e^{+\gamma_1 h} \right] = 0,$$

$$\sigma_{22F}\big|_{x_2=-h} - T_{22F}\big|_{x_2=-h} = 0 \Rightarrow \sum_{k=1}^{6} (sc_{11} + c_{13} b_k s Y_k + e_{13} b_k s Z_k) e^{-b_k sh} A_k$$

$$-\mu^{(1)}\omega\Bigg[A_7\left(\frac{4}{3}\delta_1^2 + \frac{2}{3}s^2 - R_0\right)e^{-\delta_1 h} + A_8\left(\frac{4}{3}\delta_1^2 + \frac{2}{3}s^2 - R_0\right)e^{+\delta_1 h}$$

$$+A_9\left(-s\gamma_1 - \frac{2}{3}s\gamma_1\right)e^{-\gamma_1 h} + A_{10}\left(s\gamma_1 + \frac{2}{3}s\gamma_1\right)e^{+\gamma_1 h}\Bigg],$$

$$D_{2F}\big|_{x_2=-h} = 0 \Rightarrow \sum_{k=1}^{6}\left(se_{13} + b_k s e_{33} Y_k - \varepsilon_{33}\frac{c_{44}}{e_{15}} s b_k Z_k\right)e^{-b_k sh} A_k = 0,$$

$$\left.\frac{\partial u_{1F}}{\partial t}\right|_{x_2=-h} - V_{1F}\big|_{x_2=-h} = 0 \Rightarrow -\omega\sum_{k=1}^{6} A_k e^{-b_k sh}$$

$$-\omega h\Big[-A_7 s e^{-\delta_1 h} - A_8 s e^{+\delta_1 h} + A_9 e^{-\gamma_1 h} + A_{10} e^{+\gamma_1 h}\Big] = 0,$$

$$\left.\frac{\partial u_{2F}}{\partial t}\right|_{x_2=-h} - V_{2F}\big|_{x_2=-h} = 0 \Rightarrow i\omega\sum_{k=1}^{6} A_k Y_k e^{-b_k sh}$$

$$-\omega h\Big[A_7\delta_1 e^{-\delta_1 h} - A_8\delta_1 e^{+\delta_1 h} - A_9 s e^{-\gamma_1 h} - A_{10} s e^{+\gamma_1 h}\Big],$$

$$V_{1F}\big|_{x_2=-h-h_d} = 0 \Rightarrow -A_7 s e^{-\delta_1(h+h_d)} - A_8 s e^{+\delta_1(h+h_d)} + A_9 e^{-\gamma_1(h+h_d)} + A_{10} e^{+\gamma_1(h+h_d)} = 0,$$

$$V_{2F}\big|_{x_2=-h-h_d} = 0 \Rightarrow A_7\delta_1 e^{-\delta_1(h+h_d)} - A_8\delta_1 e^{+\delta_1(h+h_d)} - A_9 s e^{-\gamma_1(h+h_d)} - A_{10} s e^{+\gamma_1(h+h_d)} = 0. \quad (34)$$

Consider the integral calculation algorithm in (18), and it is noted that these integrals are commonly known as wavenumber integrals. As a result, if we take the ratio ω/s as the velocity, the determinant (indicate as $\det||a_{nm}||$ where n, $m = 1, 2, \ldots, 10$) coincides with the left side of the corresponding dispersion equation of the wave propagating with the velocity ω/s in the system under consideration. No explicit expressions for the matrix components (a_{nm}) are given here, because they can be easily determined from the coefficient matrix of the system of equations in (34). Therefore, the unknown coefficients A_k ($k = 1, 2, \ldots, 10$) are found in the following form,

$$A_k = \frac{\det||b_{nm}^k||}{\det||a_{nm}||}, \quad (35)$$

where the matrix (b_{nm}^k) is obtained from the matrix (a_{nm}), then by replacing the kth column of the latter with the column $(0, 0, -P_0 / c_{44}, 0, 0, 0, 0, 0, 0)^T$. Note that the equation ($\det||a_{nm}|| = 0$) has a certain number of roots with respect to s for each chosen ω. It should be noted that these roots are complex numbers when at least one of the system constituents is time-dependent. Otherwise, these roots are real numbers, which makes direct calculation of the wavenumber integrals in (18) using the corresponding well-known traditional algorithms significantly more difficult. In such cases, the Sommerfeld contour method for calculating wavenumber integrals is used, as discussed and used in the monograph (Akbarov 2015) and the works reviewed in (Akbarov 2018). In this case, the integrals in (18) can be calculated using the well-known Gauss integration algorithm. In this calculation procedure, we return to the relation $g(x_1, x_2, t) = \bar{g}(x_1, x_2)e^{i\omega t}$ and the originals of the sought values are determined from the relation

$$\{\sigma_{22}, \sigma_{12}, \sigma_{11}, D_1, D_2, \varphi, u_1, u_2, T_{22}, T_{12}, T_{11}, V_1, V_2\}$$

TABLE 1. Mechanical, piezoelectric, and dielectric constants of selected piezoelectric materials [23, 24]

Materials	$c_{44}\times10^{-10}$, N/m^2	$c_{11}\times10^{-10}$, N/m^2	$c_{13}\times10^{-10}$, N/m^2	$c_{33}\times10^{-10}$, N/m^2	ρ, kg/m^3
PZT-2	2.22	13.5	6.81	11.3	7600
PMN-%28PT	6.49	19.96	7.19	15.36	8102
Materials	e_{31}, C/m^2	e_{33}, C/m^2	e_{15}, C/m^2	$\varepsilon_{11}\times10^{-9}$, F/m	$\varepsilon_{33}\times10^{-9}$, F/m
PZT-2	–1.9	9.0	9.8	8.7	3.9
PMN-%28PT	3.43	15.74	16.74	0.66	0.56

$$= \frac{1}{2\pi}\mathrm{Re}\left\{ e^{i\omega t}\int_{-\infty}^{\infty}[\sigma_{22F},\sigma_{12F},\sigma_{11F},D_{1F},D_{2F},\varphi_F,u_{1F},u_{2F},T_{22F},T_{12F},T_{11F},V_{1F},V_{2F}]e^{isx_1}\,ds\right\}. \quad (36)$$

Moreover, note that under the calculation procedure, the improper integrals $\int_{-\infty}^{\infty} f(s)\cos(sx_1)ds$ and $\int_{-\infty}^{\infty} f(s)\sin(sx_1)ds_1$ which follow from the integrals in (41) are replaced by the corresponding definite integrals $\int_{-S_1^*}^{S_1^*} f(s)\cos(sx_1)ds$ and $\int_{-S_1^*}^{S_1^*} f(s)\sin(sx_1)ds_1$, respectively, and the values of S_1^* are determined from the convergence requirement of the numerical results. After this replacement, the integration interval $[-S_1^*, S_1^*]$ is divided into a certain number of shorter intervals which are used in the Gauss integration algorithm. However, when the fluid is modeled as inviscid, the integrals are evaluated using the Sommerfeld contour method.

The boundary value problem has been effectively solved using the exponential Fourier transform in order to get an analytical solution. After obtaining the transforms of desired values, the original values have been found numerically from the relation given in (36). All these calculations are performed automatically with the PC programs in MATLAB.

4. Calculation Results. In this research, the numerical results are obtained for the piezoelectric materials whose properties are given in Table 1. Glycerin with the viscosity coefficient $\mu^{(1)} = 1.393\,\mathrm{kg/(m\cdot s)}$, density $\rho_0^{(1)} = 1260\,\mathrm{kg/m^3}$, and sound speed $a_0 = 1927\,\mathrm{m/s}$ is chosen as the fluid (Guz 2009). All numerical results shown in this study are obtained for stress acting on the interface plane between the piezoelectric plate and fluid. The primary focus of this paper is the effect of the fluid viscosity on the interface stress quantities. Furthermore, the effect of the fluid viscosity on stress in the interface plane is investigated for various plate materials. At the same time, the effect of the vibration phase on the investigated stress value is considered. And at last, for different h_d / h ratio, the interface frequency response curves of the fluid in viscous and inviscid fluid states are examined.

The numerical results in Fig. 2 show the influence of the fluid viscosity on the frequency response of the dimensionless interface normal stress $T_{22}h/P_0$ calculated at the point $x_1/h = 0$.

The numerical results shown in Figs. 2*a–c* indicate that the absolute values of the interface pressure decrease as the fluid depth increases, i.e. with ratio h_d / h. Additionally, it can be seen that the pressure value rises as the plate thickness increases by comparing Figs. 2*a* and 2*d*. Fluid viscosity causes the absolute value of the interface pressure to increase. Also, the difference between the influence of viscous and inviscid fluid on pressure reduces as the ratio h_d / h rises. Fluid viscosity, on the other hand, has greater effect on the stress value of the PMN-PT material than the PZT-2 material.

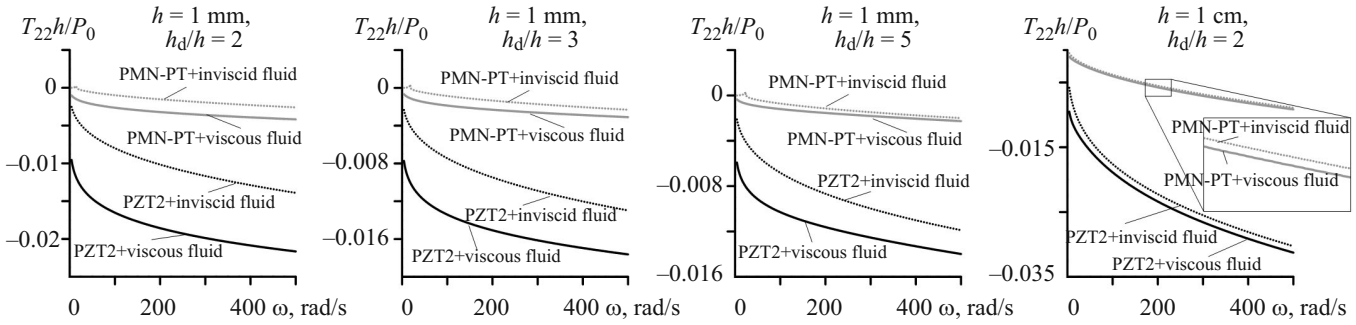

a *b*

Fig. 2. Frequency responses of interface normal stress of PZT-2 and PMN-PT plate materials in case of viscous and inviscid fluid interactions.

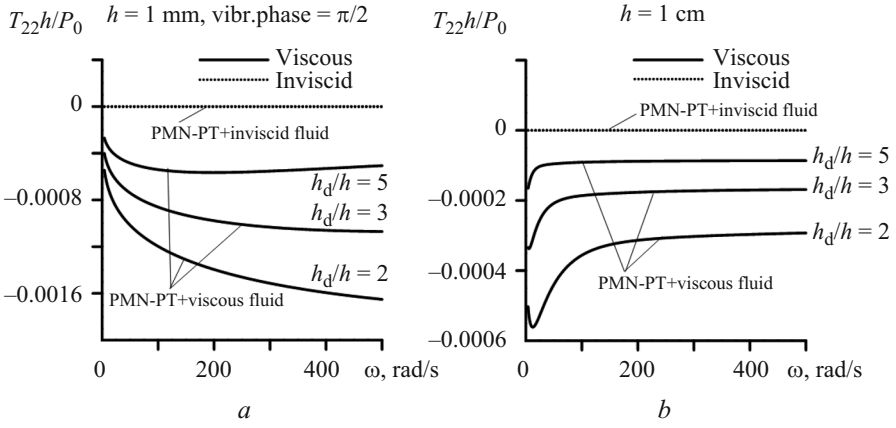

a *b*

Fig. 3. Frequency response of interface stress for PMN-PT in case of viscous and inviscid fluid interactions under $\omega t = \pi / 2$.

Figure 3 shows the stress values of the PMN-PT plate material and the viscous/non-viscous fluid interface plane when the vibration frequency is taken as $\pi / 2$. As can be seen, when the vibration phase is $\pi / 2$, there is quite a decrease in the absolute value of the stress value.

When comparing Fig. 2 and Fig. 3, the stress values decrease for both inviscid and viscous fluid cases. In Fig. 3, while the stress value for inviscid fluids is almost zero, the stress value for viscous fluids has decreased by six times compared to the vibration phase, which is equal to zero.

The curves showing the relationship between the interface stress value and the vibration frequency of the PMN-PT plate material are given in Fig. 4. The curves given in Fig. 4*a-c* are constructed for the cases with respect to the ratio h_d / h for the plate under $\omega = 400$ (rad/s) and $h = 0.001$ m, $h = 0.01$ m, and $h = 0.0001$ m, respectively.

These figures show that it is valid for all plate thickness values and all h_d / h ratios where the fluid viscosity causes the increase above the interface stress value. Also, the fluid viscosity can significantly shift the vibration phase at which the studied stress has its absolute minimum value. According to Fig. 4, it can be seen that the shifting effect of the fluid viscosity on the vibration phase decreases when the plate thickness increases.

5. Summary and Conclusions. This article is devoted to the investigation of the mechanically forced vibration of the hydro-piezoelectric system consisting of a piezoelectric plate, a compressible viscous fluid and a rigid wall. The PZT layer of the plate is assumed to be in contact with the fluid and the time-harmonic linear forces act on the free surface of the elastic-metallic layer. The plate motion is described using the exact equations and relations of elasto-electrodynamics for the piezoelectric materials within the piecewise homogeneous body model. The fluid flow is described by the linearized Navier-Stokes equations for the barotropic compressible viscous Newtonian fluid. Besides, the fluid equations have been rewritten as above for cases where the fluid is inviscid. The plane-strain state in the plate and the plane flow in the fluid occur. The Fourier transform is used with respect to the spatial coordinate on the axis along the plate laying direction in order to solve the corresponding boundary-value problem. The analytical expressions of the Fourier transform for all sought values of each component of the system are determined.

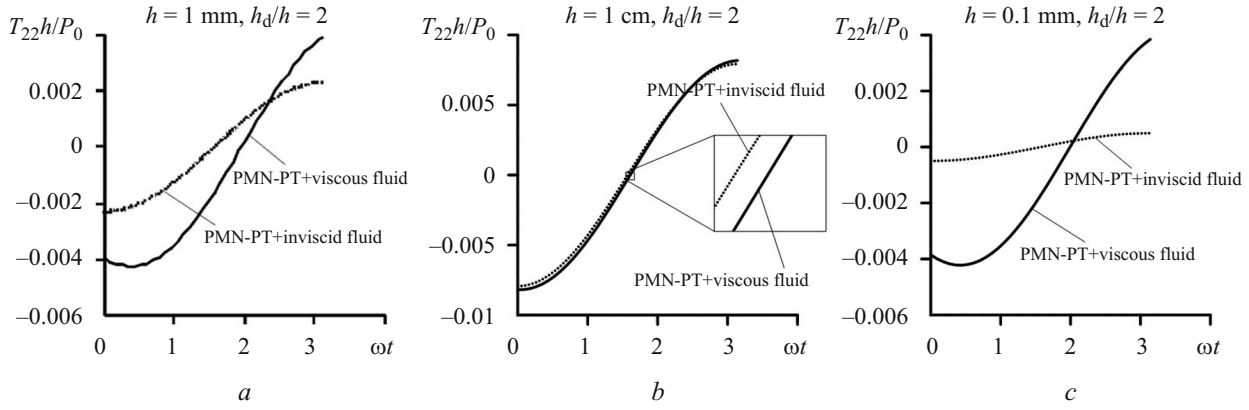

Fig. 4. Curves of dependence between interface stress and vibration phase for PMN-PT in case of viscous and inviscid fluid interactions.

These results are obtained by selecting PMN-PT and PZT-2 as piezoelectric materials and glycerin as fluid. The analysis of these results allows for the following conclusions about the influence of the fluid viscosity on the frequency response of the stress acting on the interface between the piezoelectric layer and fluid:

For all plate materials and fluid states, the absolute values of the interface pressure decrease as the fluid depth increases, i.e., with the ratio h_d / h.

Fluid viscosity raises the absolute value of the interface pressure, as seen in all figures.

The difference between the interface pressure values of viscous and inviscid fluids decreases as the h_d / h ratio increases.

The amount of difference between the interface stress values of viscous fluid and inviscid fluid states can change according to the type of the piezoelectric plate.

The vibration phase is shown to be important in the plate-viscous-inviscid fluid interaction problem. The interface stress approaches zero in the case of inviscid fluid when the fluid phase is taken as $\pi / 2$.

When the vibration phase is $\pi / 2$, the interface stress value in the viscous fluid-plate interaction decreases compared to when the vibration phase is 0.

Fluid viscosity can significantly shift the value of the vibration phase at which the interface stress has its absolute minimum.

REFERENCES

1. H. Lamb, "Axisymmetric vibration of circular plates in contact with water," *Proc. R. Soc. Lond. A*, **98**, 205–216 (1921).
2. M. Amabili and M. K. Kwak, "Free vibrations of circular plates coupled with liquids: revising the Lamb problem," *J. Fluids Struct.*, **10**, No. 7, 743–761 (1996).
3. S. D. Akbarov, "Forced vibration of the hydro-viscoelastic and elastic systems consisting of the viscoelastic or elastic plate, compressible viscous fluid and rigid wall: a review," *Appl. Comput. Math*., **17**, No. 3, 221–245 (2018).
4. S. D. Akbarov and M. I. Ismailov, "The forced vibration of the system consisting of an elastic plate, compressible viscous fluid and rigid wall," *J. Vib. Control*, **23**, No. 11, 1809–1827 (2017).
5. A. N. Guz, *Dynamics of Compressible Viscous Fluid*, Cambridge Scientific Publishers, Cottenham (2009).
6. A. N. Guz, A. P. Zhuk, and A. M. Bagno, "Dynamics of elastic bodies, solid particles, and fluid parcels in a compressible viscous fluid (Review)," *Int. Appl. Mech.*, **52**, No. 5, 449–507 (2016).
7. V. N. Paimushin and R. K. Gazizullin, "Free and forced vibrations of a composite plate in a perfect compressible fluid, taking into account energy dissipation in the plate and fluid," *Lobachevskii J. Math.*, **42**, No. 8, 2016–2022 (2021).
8. V. N. Paimushin, D. V. Tarlakovskii, V. A. Firsov, and R. K. Gazizullin, "Free and forced bending vibrations of a thin plate in a perfect compressible fluid with energy dissipation taken into account," *Z. Angew. Math. Mech*., e201900102 (2020).

9. M. Shuaib, M. Bilal, M. A. Khan, and S. J. Malebary, “Fractional analysis of viscous fluid flow with heat and mass transfer over a flexible rotating disk,” *Comput. Model. Eng. Sci.*, **123**, No. 1, 377–400 (2020).
10. S. V. Sorokin and A. V. Chubinskij, “On the role of fluid viscosity in wave propagation in elastic plates under heavy fluid loading,” *J. Sound Vib.*, **311**, 1020–1038 (2008).
11. A. D. Zamanov, M. I Ismailov, and S. D. Akbarov, “The effect of viscosity of fluid on the frequency response of a viscoelastic plate loaded by this fluid,” *Mech. Compos. Mater.*, **54**, No. 1, 41–52 (2018).
12. K. Jeong and K. Kim, “Hydroelastic vibration of a circular plate submerged in a bounded compressible fluid,” *J. Sound Vib.*, **283**, Nos. 1–2, 153–172 (2005).
13. M. E. Yildizdag, I. T. Ardic, M. Demirtas, and A. Ergin, “Hydroelastic vibration analysis of plates partially submerged in fluid with an isogeometric FE-BE approach,” *Ocean Eng.*, **172**, 316–329 (2019).
14. C. Y. Liao and C. C. Ma, “Vibration characteristics of rectangular plate in compressible inviscid fluid,” *J. Sound Vib.*, **362**, 228–251 (2016).
15. K. Khorshidi, M. Karimi, M. Bahrami, M. Ghasemi, and B. Soltannia, “Fluid-structure interaction analysis of vibrating microplates in interaction with sloshing fluids with free surface,” *Appl. Ocean Res.*, **121**, 103088 (2022).
16. S. D. Akbarov and E. T. Bagirov, “Dispersion of the axisymmetric waves propagating in the hydro-elastic system consisting of the pre-strained highly elastic plate, compressible inviscid fluid, and rigid wall,” *Arch. Appl. Mech.*, **93**, 861–879 (2023).
17. V. S. Popov, et al., “Hydroelastic response of an end wall interacting with a vibrating stamp via a viscous liquid layer,” *J. Phys.: Conf. Ser.*, **1441**, 012108 (2020).
18. D. V. Kondratov, et al., “Mathematical modeling of circular sandwich plate interaction with viscous liquid layer for predicting its hydroelastic response,” *J. Phys.: Conf. Ser.*, **1784**, 012005 (2021).
19. S. D. Akbarov and T.V. Huseynova, “Forced vibration of the hydro-elastic system consisting of the orthotropic plate, compressible viscous fluid and rigid wall,” *Coupled Syst. Mech.*, **8**, No. 3, 199–218 (2019).
20. B. Liu, Q. Jiang, and J. Yang, “Fluid-induced frequency shift in a piezoelectric plate driven by lateral electric fields,” *Int. J. Appl. Electrom.*, **34**, No. 3, 171–180 (2010).
21. S. Sorokin, and A. Chubinskij, “On the role of fluid viscosity in wave propagation in elastic plates under heavy fluid loading,” *J. Sound Vib.*, **311**, Nos. 3–5, 1020–1038 (2008).
22. Z. E. Kuzeci and S. D. Akbarov, “The influence of the coupling effect of physical-mechanical fields on the forced vibration of the hydro-piezoelectric system consisting of a PZT layer and a viscous fluid with finite depth,” *Struct. Eng. Mech.*, **85**, No. 2, 247–263 (2023).
23. J. Yang, *An Introduction to the Theory of Piezoelectricity*, Springer, New York (2005).
24. M. Shanthi, L. C. Lim, K. K. Rajan, and J. Jin, “Complete sets of elastic, dielectric, and piezoelectric properties of flux-grown [011]-poled $Pb(Mg_{1/3}Nb_{2/3})O_3$-(28–32)% $PbTiO_3$ single crystals,” *Appl. Phys. Lett.*, **92**, No. 14, 142906 (2008).